

How Air Voids Affect the Performance of Concrete Subjected to Fire

Yu Chen

A thesis

submitted in partial fulfillment of the
requirements for the degree of

Master of Science in Construction Management

University of Washington

2019

Reading Committee:

Kamran M. Nemati, Chair

Yong Woo Kim

Program Authorized to Offer Degree:

Construction Management

© Copyright 2019

Yu Chen

University of Washington

Abstract

How Air Voids Affect the Performance of Concrete Subjected to Fire

Yu Chen

Chair of the Supervisory Committee:
Associate Professor Kamran M. Nemati
Department of Construction Management

Spalling is a hazardous phenomenon that structures will experience during a fire. It has been extensively studied recent years. Inclusion of polypropylene fibers in concrete mix are commonly treated as a feasible method against spalling as they can increase the permeability of concrete in high temperature environments to release the interior pressure. Recently, air entrained concrete is thought to be a suitable alternative to polypropylene fiber reinforced concrete under fire conditions. The fundamental point of this study is to identify how the percentage of air voids, and the combination of polypropylene fibers and air entraining admixture can affect the permeability of concrete and therefore the occurrence of spalling phenomenon. For this reason, twelve mixes of concrete with different water to cement ratios, and

various polypropylene fibers and air void content were produced. Fire experiment were carried on the specimens using a standard ASTM E-119 fire curve for the duration of 90 minutes, reaching 1850 °F in a furnace. In this study compressive strength, mass loss and photographic documentation of specimens were investigated and compared. Results show that addition of air entraining admixture helps reduce compressive strength loss, but the trend was found to be irregular.

TABLE OF CONTENTS

List of Figures	iii
List of Tables	iv
Chapter 1. Introduction	1
Chapter 2. Literature review	4
2.1 Mechanical Properties.....	4
2.1.1 General.....	4
2.1.2 Previous Studies.....	5
2.1.3 Effect of Temperature on Mechanical Properties of Concrete	8
2.2 Spalling.....	8
2.2.1 General.....	8
2.2.2 Previous Studies.....	8
2.2.3 Spalling mitigation.....	10
2.2.4 Summary.....	12
Chapter 3. Experimental program.....	14
3.1 Test material.....	14
3.2 Mix proportions and test specimens	14
3.3 Test equipment.....	15
3.4 Heating procedure.....	17
3.5 Test conditions and procedure	17
3.5.1 Compressive strength measurement	18

3.5.2	Mass loss measurement.....	18
Chapter 4. Data analysis and Discussion		19
4.1	Compressive strength.....	19
4.2	Mass loss.....	22
4.3	Effect of PP fibers.....	25
4.4	Visual observation of the specimens.....	27
4.5	Comparison of compressive strength and mass loss with other studies	29
4.6	Discussion.....	34
Chapter 5. Conclusion and recommendation		39
Bibliography		41

LIST OF FIGURES

Figure 3.1. Demonstration of the furnace (Fantilli et al., 2018)	16
Figure 3.2. Placement of the specimens (Fantilli et al., 2018).....	16
Figure 3.3. Time-temperature curve ASTM E-119 (ASTM E-119).....	17
Figure 4.1. Compressive strength (MPa) – Air content (%) at room temperature.....	20
Figure 4.2. Residual compressive strength (MPa) – Air content (%) after heating.....	21
Figure 4.3. Relative compressive strength (%) – Air content (%) after heating.....	22
Figure 4.4. Mass loss (%) – w/c (%).....	24
Figure 4.5. Mass loss (%) – Air content (%)	25
Figure 4.6. Mass loss (%) – Air content (%)	26
Figure 4.7. Residual compressive strength (MPa) – Air content (%) after heating.....	26
Figure 4.8. Relative compressive strength (%) – Air content (%) after heating.....	27
Figure 4.9. Photographic documentations of specimens after heating (Fantilli et al., 2018)29	
Figure 4.10. Variation in residual compressive strength as function of temperature (Waheed et al., 2018)	31
Figure 4.11. Relative mass loss after exposure to different temperatures in air and non-air entrained HSC (Waheed et al., 2018)	31
Figure 4.12. TGA and DTG curves (Akca and Zihnioğlu, 2013).....	32
Figure 4.13. (a) A PP fiber passing through an air void, (b) a micro-channel formed after heating (a part of a melted PP fiber reaches to an entrained air void creating a micro-channel) (Akca and Zihnioğlu, 2013).....	34
Figure 4.14. Compressive strength (MPa) – Air content (%) at room temperature.....	35
Figure 4.15. Residual compressive strength (MPa) – Air content (%) after heating.....	36
Figure 4.16. Relative compressive strength (%) – Air content (%) after heating.....	36
Figure 4.17. Mass loss (%) – Air content (%)	37

LIST OF TABLES

Table 3.1. Properties of polypropylene fibers.....	14
Table 3.2. Characteristics of twelve mixes	15
Table 4.1. Average initial and residual compressive strength values	19
Table 4.2. Average mass loss values	23
Table 4.3. Average compressive strength and mass loss values.....	25

ACKNOWLEDGEMENTS

I would like to express my greatest appreciation to my advisor, Prof. Kamran M. Nemati, University of Washington, who has given me great support, patient and guidance, and shared his experimental data. During my years of graduate study at University of Washington, he has shared his creative ideas, skills and perseverance which made my graduate studies very rewarding.

I would also like to thank Prof. Yong Woo Kim joining supervisor committee, and for their valuable advice throughout my graduate study at University of Washington.

I would like to thank my mom Li Liu, my father You Nian Chen, my friends Zhen wei Ma, Zi Yang Xiao, Shuo Chen for their constant support and encouragement throughout these years.

I would like to thank JJ Lin for giving me spiritual support with his beautiful songs.

Finally, I would like to thank all the faculty members and students at University of Washington for giving me help and support during my graduate studies.

Chapter 1. INTRODUCTION

Fire is one of the most severe hazards a structure can suffer during its lifetime. Therefore, providing fire protection methods is a significant aspect of building design. The fire protection measures could include active and passive systems, and the main purposes are to control the spread of fire and ensure the safety of the occupants. Once a fire happens, active systems are usually activated automatically, including fire detectors, smoke control systems, and sprinklers. Passive systems are built into buildings and could be achieved by structural members' fire resistance. "Fire resistance is defined as the duration during which a structural member exhibits resistance with respect to structural integrity, stability, and temperature transmission when exposed to fire (Khaliq, 2012)."

Concrete is non-combustible and has excellent fire resistance in many cases and can help prevent structural breakdown when subjected to fire. It is an ideal solution for building safety and has become one of the most widely used building materials because of its excellent strength, durability and fire resistance. However, as concrete is complex and heterogeneous, its thermal and mechanical properties tend to change in an irreversible process when being exposed to high temperatures, which could reduce its fire resistance. Spalling, defined as small pieces of concrete fall from its surface, is a hazardous phenomenon that it will experience during a fire. This phenomenon could cause detachment of concrete which will result in exposing reinforcing bar to high temperatures, thereby significantly reducing structures' load-bearing capacity.

Research and development have shown that there can be different methods for increasing the fire resistance of concrete, such as modification of mix design by incorporating different types of fibers and improvement in design of member dimensions. Increasing concrete permeability

achieved by incorporation of polypropylene (PP) fibers could be a viable solution. As these fibers melt in the temperature range of 160 – 170 °C depending on its molecular structure, pores and vacant channels created by melting of these fibers allows the release of high vapor pressure developing inside concrete due to high temperature. This could help mitigate spalling.

Admixtures are products that are often incorporated at low dosage in concrete mixtures in order to modify properties of concrete. The admixtures can be classified into three types: First, mineral admixtures that are used to improve workability and durability such as fly ash. Second, set-controlling chemicals that are used to affect setting time or strength development rate such as accelerating admixture. Third, surface-active chemicals that are often used for the purpose of air entrainment or water reduction such as air entraining admixture (AEA) (Mehta and Monteiro, 2014). AEA are often used against freeze-thaw damage, as AEA create air voids inside concrete which provide places for water to storage without damaging the structure. As pore pressure is one of the factors that could lead to spalling, it is hypothesized that air voids created by AEA could help reduce pore pressure. Thus, AEA could be an alternative to PP fibers. Moreover, Air entrained concrete could provide enhanced workability and porosity. However, due to lack of research, it is hard to evaluate the fire performance of air entrained concrete. To overcome the current knowledge gaps, this research is aimed at addressing the following objectives:

I) Undertake a detailed literature review on the high temperature properties of concrete. This review will include experimental studies on thermal and mechanical properties of concrete, fire induced spalling and methods to overcome spalling.

II) Undertake fire test on concrete to recognize fire performance of air entrained concrete and identify improvements offered by AEA through controlling air void system.

III) Undertake fire test on concrete to compare fire resistance of fiber-reinforced concrete and air entrained concrete.

Chapter 2. LITERATURE REVIEW

2.1 MECHANICAL PROPERTIES

2.1.1 *General*

When considering fire resistance design for concrete structure, the mechanical properties of concrete, such as compressive and tensile strengths, play an important role. Lea (1920) investigated the effect of high temperature on concrete strength. Since then, researchers have studied mechanical properties of concrete at elevated temperatures.

Concrete compressive strength depends upon several factors such as water/cement ratio, curing conditions, aggregate type and size, and type of stress (Mehta and Monteiro, 2014). Compared to compressive strength, the tensile strength is much lower.

There are three test methods to determine the mechanical properties of concrete at high temperature: stressed test, unstressed test, and residual test (Khaliq, 2012). When using stressed test, specimens are preloaded to a specific load before being exposed to elevated temperature. In unstressed test, specimens are exposed to the desired temperature without load. Once target temperature is reached, specimens are loaded to failure. These two test methods are used for acquiring the strength at high temperatures, while the residual test is suitable for obtaining the residual mechanical properties after being exposed to high temperatures. As the result of decomposition and dehydration taking place inside concrete (Liu et al., 2018), the residual strength test could give the lowest strength.

2.1.2 *Previous Studies*

2.1.2.1 Compressive Strength

As mentioned above, factors such as water/cement ratio, curing conditions and aggregate type and size could influence concrete compressive strength. Considerable research about concrete compressive strength at elevated temperatures have been carried out, and a few of them are presented here.

Chan et al. (1999) studied the residual compressive strength of both normal-strength concrete (NSC) and high-strength concrete (HSC) after exposure to high temperatures. They measured strength for three temperature ranges of 20 to 400 °C, 400 to 800 °C, and 800 to 1200 °C. For NSC, only 15% of strength was lost in 20 to 400 °C. Severe loss of strength happened in 400 to 800 °C due to the deterioration of calcium silicate hydrate (CSH) gel and dehydration in concrete which results in loss of cementing ability. This temperature range was suggested to be critical to concrete strength loss. When concrete was exposed above 800 °C, a small part of compressive strength was left, and concrete was structurally damaged.

Poon et al. (2001) experimentally compared the strength of NSC and high-strength pozzolanic concrete. They identified several temperature ranges that showed distinct patterns of strength loss. From 20 to 200 °C, high-strength pozzolanic concrete showed strength increase while a small part strength loss was observed in NSC. From 200 to 400 °C, the coarsening of pore structure happened, which causes some pore volumes change, and the maximum of the differential pore volumes distribution becomes lower while the total pore volume does not increase (Rostasy, 1980). Because of pore structure coarsening, NSC experienced a 19 – 26% of original strength loss. From 400 – 600 °C, both NSC and HSC had significant strength loss (44% for HSC and 60% for NSC). When

the temperature reached above 800 °C, all specimens suffered severe deterioration due to the decomposition of CSH gel. The final residual strengths were 17% of original strength for NSC and 26% for HSC. NSC was observed to experience a gradual decrease in strength, while HSC showed sharp strength decrease between 400 and 800 °C.

Noumowé et al. (2009) investigated the characteristics of concrete exposed to temperature up to 310 °C. The observed strength loss was minor between 20 and 110 °C. From 210 °C, significant strength loss was observed, and the strength loss was 36% at 310 °C. They also did the comparative study about aggregate type and suggested that concretes made with limestone aggregates show comparable results.

Behnood and Ghandehari (2009) made a comparison of concrete with and without PP fibers at high temperature. For concretes without PP fibers, they tested the compressive strength at 20, 100, 200, 300, 600 °C. After heating to 100 °C, all non-fibrous specimens showed strength decrease between 14% and 16%. Compared to 100 °C, all non-fibrous specimens experienced a slight increase in residual strength at 200 °C. Due to the moisture content vaporize at high temperature, the increase in strength was suggested to results from the increase in surface forces between gel particles (Van der Waals forces). In the temperature range 300 to 600 °C, all specimens suffered significant strength decrease. After exposed to 600 °C, the residual strength of NSC was about 32%.

2.1.2.2 Tensile Strength

Concrete tensile strength can be tested using three methods: flexural tensile, direct tensile and splitting tensile. Several factors could impact tensile strength such as compressive strength,

water/cement ratio, and microstructure of concrete (Khaliq, 2012; Neville, 1963). Some of the previous studies are presented here.

Carette et al. (1982) investigated the temperature effect on concrete cylinders in temperature between 75-600 °C. After heating to 600 °C, concrete experienced 50-65% tensile strength loss. They suggested that water/cement ratio and aggregate type had a significant impact on concrete tensile strength in high temperature.

Chan et al. (1999) indicated that unlike the gradual loss of compressive strength, concrete experienced sharp loss of tensile splitting strength when exposed to elevated temperature. They suggested that it was because tensile strength was more sensitive to cracks than compressive strength.

Noumowé et al. (2009) found that splitting tensile strength loss was small at 100 °C and became significant after 210 °C. The average splitting tensile strength was 13% at 210 °C and 35% at 310 °C.

Khaliq and Khan (2015) investigated the high temperature properties of calcium aluminate cement concrete (CACC). The tensile strength loss of CACC was gradual and almost linear. NSC has similar trend till 400 °C. Above 400 °C, NSC experienced sharp loss in tensile strength which is different from CACC. However, both NSC and CACC suffered significant tensile strength loss beyond 600 °C. At 800 °C, CACC tensile strength was 1.54 times higher than NSC.

Cülfik and Özturan (2010) used image analysis to detect bond deteriorations when concrete was exposed to high temperature. After heating to 250 °C, splitting tensile strength loss reached up to 37% for NSC, while splitting tensile strength did not decrease much with increasing

temperature for NSC with silica fume. They suggest that the addition of silica fume resulted in more CSH gel formation which made a stronger bond between aggregate and cement paste.

Sideris and Manita (2013) investigated residual mechanical properties of self-compacting concrete (SCC). The relative splitting tensile strength reduced up to 300 °C, and both SCC and NSC had the similar patterns. NSC suffered spalling when the temperature is above 300 °C.

2.1.3 *Effect of Temperature on Mechanical Properties of Concrete*

The review of previous studies shows that there are variations in reported mechanical properties. These variations could be related to test procedures, test techniques and other factors such as moisture content, aggregate type, heating rates and maximum test temperature. Despite these variations, there is general agreement between researchers that concrete relative residual strength will suffer significant reduction above 400 °C.

2.2 SPALLING

2.2.1 *General*

When concrete is exposed to high temperature, small pieces of concrete fall from the surface of the concrete, which is defined as spalling. When concrete experiences fire or other thermal environmental conditions, different types of water vaporize, and temperature gradients appear. As a result, internal stresses are built up. When the internal stresses exceed the tensile strength of concrete, spalling occurs.

2.2.2 *Previous Studies*

Liu et al. (2018) compiled common views from previous works and proposed a unified spalling theory. They concluded three spalling mechanisms. The first is thermo-hygral spalling

which is known as pore pressure spalling. As temperature rises, water will be released into micropores of concrete, and pore pressure gradually develops. Pressure gradient will induce moisture to move to two opposite directions, the heated region and the cooler region, which leads to the generation of three zones. When the pressure exceeds concrete tensile strength of concrete, spalling occurs. The second is thermo-mechanical spalling which is restrained thermal dilatation (Kodur, 2000). When concrete is exposed to high temperature, temperature gradients develop which leads to the exterior surface layer of concrete experience a triaxial tension-compression-compression stress state. Compressive stress will move inward, and this process will repeat as the conditions are met until the stress reaches the interface between concrete cover and core. When the stress exceeds the concrete tensile strength, vertical cracks will form between concrete cover and core, and stress is released by brittle fracture. The third is thermo-chemical spalling which is used to explain post-cooling spalling. When concrete is exposed to high temperature, calcium carbonate decarbonates and produces calcium oxide. After cooling down, heated concrete absorb moisture in the air. The absorbed moisture will react with calcium oxide which leads to volume expansion. Due to rehydration, concrete will suffer severe spalling.

Phan (2008) investigated pore pressure and explosive spalling using set of experimental measurements. Noticeable pore pressure rise occurs when temperature reaches range of 105 to 160 °C due to the vaporization of free water. The release of chemically bound water which happens in temperature range of 160 to 180 °C leads to a sharp pressure increase. After 180 °C, pressure increases with a small rate. The peak pore pressure occurs between 220 and 245 °C. Explosive spalling occurs, and the pore pressure is measured at 2.1 MPa.

Zhao et al. (2017) investigated heating rate effect on spalling of HSC. Two types of heating conditions are used, ISO 834 standard fire ($\theta_g = 20 + 345 \log_{10}(8t+1)$) Where θ_g = temperature of

gases in the compartment in °C, t = time in minutes) and slow heating with a rate of 5 °C/min. They concluded that spalling mechanisms varied under different heating conditions. When HSC was exposed to fire heating, thermal stress spalling discussed above was the main reason. For slow heating, pore pressure spalling was the leading factor. They also inferred that if concrete could endure the temperature-gradient induced stress at the early stage when exposed to fire heating, pore pressure would then lead the process of spalling as the heating rate decreases at the late stage.

2.2.3 *Spalling mitigation*

2.2.3.1 General

Some factors such as aggregate type and density should be taken into consideration in the design of concrete mixes to minimize spalling. Some researchers have suggested adding PP fibers to concrete could alleviate spalling.

2.2.3.2 PP fibers

Khoury (2008) investigated molecular structure, materials behavior and pressure relief mechanisms of PP fibers. They propose three mechanisms of pressure relief. The first is discontinuous reservoirs. Discontinuous reservoirs include discrete bubbles and micro-cracks. Discrete bubbles are created during mixing and heating process and serve the same role as voids created by AEA. Microcracks are created around fibers. There are two possible explanations for these microcracks. One is the different thermal expansion coefficients between PP fibers and the surrounding matrix, and the other is the volumetric expansion of PP during the melting process. The second is continuous channels. Because of polarity mismatch and lack of affinity between water and PP fibers, the permeability of water through PP fibers is low. PP fibers and concrete are also dissimilar in polarity. Due to this poor interfacial adhesion, the weakly bonded space between PP fiber and concrete is vulnerable to be disrupted by vapor pressure above 100 °C, and pressure-

induced tangential space (PITS) is formed, which could serve as a pressure release route. The third is vacated channels, which is the most quoted mechanism. These channels are created by melted and vaporized PP fibers. Moreover, the vapor products are small and volatile enough to penetrate the pores in concrete and finally flow to the surface of concrete driven by pressure gradients.

Maluk et al. (2017) investigated the effects of PP fibers type and dosage on minimizing spalling. They use Heat-Transfer Rate Inducing System to study the propensity for heat-induced spalling of several concrete mixes. PP fibers with a small cross-section (i.e., 18 μ m diameter) have a negative effect on workability of concrete which leads to relative low dose of this kind of fibers should be used in concrete. PP fiber length affects minimizing spalling, as spalling occurs for all specimens with 3 mm long PP fibers. They also make comparison to examine the three mechanisms presented above. Results show that high values of total PP fibers surface area, total PP fibers length and total number of individual PP fibers have positive effect on reducing spalling. Comparison about doses of PP fibers shows that mixes with the same dose of different PP fibers have different outcome regarding spalling or not, which suggests factors other than dosage should be considered when using PP fibers to reduce spalling.

Behnood and Ghandehari (2009) compared HSC with and without PP fibers at high temperature. For compressive strength, the addition of PP fibers at different dosages does not have significant effect at 100 °C, while the presence of PP fibers noticeably increases the residual compressive strength at 200, 300, 600 °C. In case of splitting tensile strength, the presence of PP fibers is more effective than compressive strength.

2.2.3.3 Air void system

As air and water do not mix, air bubbles could generate voids inside concrete. These bubbles could vary in size and shape. During the mixing phase, these bubbles move freely, and some can be eliminated during the vibration process. Mielenz et al. (1958) have done research to identify the origin and evolution of the air void system. They concluded air voids inside concrete vary between two extremes: those that air entirely enclosed among aggregate particles and those that air enclosed by the paste composed of aggregate fines and cement. Large voids could do harm to concrete while small voids benefits concrete mainly in increasing the workability and resistance to freeze-thaw damage. People proactively create small voids inside concrete by adding AEA to obtain these benefits and this concrete is called air entrained concrete. As discussed above, PP fibers could increase permeability to increase fire resistance. However, the addition of PP fibers could greatly reduce the slump. Thus, extra efforts during casting and compaction are needed. As the permeability increase could also be achieved by AEA, air entrained concrete could theoretically be an alternative for fire resistance application.

Air voids system is measured with two factors: spacing factor and specific surface. The spacing factor is defined as the maximum distance from the periphery of an air void to cement paste and the specific surface is referred to the total air voids surface area divided by total air volume (Waheed et al., 2018). Some researchers have done experiments to find how these two factors affect freeze-thaw durability (Pigeon et al., 1989; Siebel, 1989). However, no specific ranges of these two factors have been reported for fire resistance due to lack of research.

2.2.4 *Summary*

Spalling of concrete can be attributed to intrinsic factors such as concrete strength, density, aggregate type and moisture content, and external factors such as heating conditions and external

load (Kodur, 2000). The occurrence of spalling will severely jeopardize the strength of concrete. Therefore, spalling is a significant problem that needs to be solved when people make concrete fire resistance design.

The fire resistance design against spalling could be achieved through the increase of the permeability or the control the fracture energy. The control of water to cement ratio and the addition of different types of fibers have been reported to be reliable methods if applied correctly.

Chapter 3. EXPERIMENTAL PROGRAM

3.1 TEST MATERIAL

Type I ordinary Portland cement meeting the requirements of ASTM C 150 was used in the preparation of the concrete specimens. Natural sand from Washington State with water absorption of 1.69% and a specific gravity of 2.65 was used as fine aggregate. Coarse aggregate with maximum size of 3/4-inch was used. Its water absorption was 1% and its specific gravity was 2.68. Glenium 3030 was used as superplasticizer and AE 90 was used for AEA in concrete. PP fibers MasterFiber MAC 2200 CB were used at dosage of 2 kg/m³. Typical properties of fibers are presented in Table 3.1.

Table 3.1. Properties of polypropylene fibers

Physical properties	Values
Specific gravity (g/cm ³)	0.91
Melting point (°C)	160
Tensile strength (Ksi)	85
Length (in.)	2.1

3.2 MIX PROPORTIONS AND TEST SPECIMENS

Twelve mixes of concrete were designed and total of seventy-two specimens were casted. Tests were carried out to investigate the behavior of different concretes with water to cement ratios of 0.3, 0.4, and 0.5. Air content varied from 5% to 15%. For fiber reinforced concrete mixes, w/c was kept as 0.3 and fiber volume fraction was kept as 2 kg/m³. Characteristics of twelve different mixes are shown in the Table 3.2.

Table 3.2. Characteristics of twelve mixes

Mixture	w/c	Voids (%)	Fiber volume fraction (%)
1	0.3	5	0
2	0.3	10	0
3	0.3	15	0
4	0.3	5	2
5	0.3	10	2
6	0.3	15	2
7	0.4	5	0
8	0.4	10	0
9	0.4	15	0
10	0.5	5	0
11	0.5	10	0
12	0.5	15	0

By varying the air content, it is possible to analyze whether increasing air voids could help increase the resistance to spalling phenomenon.

The specimens were cylinders with 300 mm (12 inches) height and 150 mm (6 inches) diameter and were produced in the Seattle Concrete Lab of Lafarge.

3.3 TEST EQUIPMENT

The fire laboratory of Worcester Polytechnic Institute (WPI) in Massachusetts was used to conduct the fire experiments on twenty-four specimens (A series and B series). The furnace used in this experiment is shown in Figure 3.1 and has dimensions as $1.60 \times 1.60 \times 1.00$ m. To avoid heat loss on hot specimens, insulation coverings, designed to withstand temperature above 1800 °F, were used to completely insulate the interior of the furnace. Internal thermocouple inside a ceramic pipette was used to monitor the furnace temperature. There were two burners in upper and lower wall of the furnace and each one consists of 38 outputs. The operating center for ignition and temperature modulation was in the back of the furnace. The capacity of the furnace was four

specimens for each run. Four specimens were placed on the corners to prevent being hit directly by the burners (Figure 3.2). For each specimen, four thermocouples connected to a computer were used to measure the surface temperature and the temperatures were recorded with the frequency of a second.



Figure 3.1. Demonstration of the furnace (Fantilli et al., 2018)



Figure 3.2. Placement of the specimens (Fantilli et al., 2018)

3.4 HEATING PROCEDURE

The heating rate was set to follow the time-temperature curve according to the ASTM E-119 standard (Figure 3.3). The total duration of the experiment was 90 minutes and the corresponding temperature was 1792 °F. The reached maximum temperature in the furnace was 1850 °F.

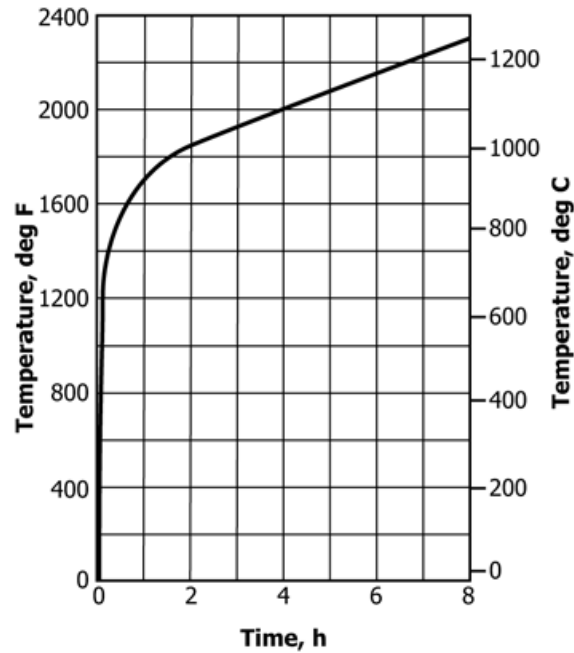


Figure 3.3. Time-temperature curve ASTM E-119 (ASTM E-119)

At the end of the heating period, the hot concrete specimens were not taken out immediately in order to avoid creating thermal shocks. After heating was stopped and the temperature was lower than 1100 °F, the door was opened slightly to facilitate the cooling of the furnace. The door was completely opened when the temperature reached 500 °F.

3.5 TEST CONDITIONS AND PROCEDURE

Mass measurements and compressive strength tests were carried out on concrete specimens before and after heating.

3.5.1 *Compressive strength measurement*

Standard test procedure following ASTM C 39 for compressive strength was used to evaluate the high-temperature properties of concrete specimens. As the specimens were brittle after being exposed to high temperature, a lower load increase compared to a normal compression test, 1100 psi / min (7.5 MPa / min), was used.

3.5.2 *Mass loss measurement*

Mass of specimens were measured before heating test and measured again when the specimen cooled down to room temperature after heating. During the heating period, moisture in the test specimens was allowed to escape freely.

Chapter 4. DATA ANALYSIS AND DISCUSSION

The experimental test results obtained from compressive strength and mass loss tests are discussed in this section.

4.1 COMPRESSIVE STRENGTH

The compressive strength suffer slight reduction up to 100 °C. In this temperature range, the main reason for strength loss is the loss and vaporization of free and adsorbed water. When temperature reaches higher than 400 °C, significant compressive strength loss occurs. Because of thermal incompatibility of aggregates and CSH gel, aggregate-paste bond deteriorates. Disintegration of CSH gel, decomposition of calcium hydroxide which mainly occurs between 400 and 600 °C, decarbonation of calcium carbonate which mainly occurs between 600 and 800 °C, all these factors contribute to this significant strength loss. Test results are shown in Table 4.1. It can be observed that all specimens were extremely fragile with 6 -8 % compressive strength left. The residual compressive strength values vary from a minimum of 3.44 MPa and a maximum of 5.57MPa.

Table 4.1. Average initial and residual compressive strength values

Mixes	w/c	Void (%)	Initial strength		Residual strength		
			(MPa)	(psi)	(MPa)	(psi)	(%)
1	0.3	5	69.1	10017.9	5.6	808.5	8.1
2	0.3	10	45.5	6598.3	3.5	504.9	7.7
3	0.3	15	57.7	8368.4	4.5	647.9	7.7
7	0.4	5	64.8	9397.0	3.9	568.5	6.0
8	0.4	10	56.9	8259.8	5.0	731.9	8.9
9	0.4	15	50.4	7313.2	4.3	619.8	8.5
10	0.5	5	48.9	7092.5	4.3	617.0	8.7
11	0.5	10	42.7	6197.7	3.4	498.7	8.0

12	0.5	15	41.7	6053.2	2.9	424.9	7.0
----	-----	----	------	--------	-----	-------	-----

From Figure 4.1, it could be observed that AEA addition affects compressive strength at room temperature. With the increase of air content, compressive strength decreases. One exception is the specimens with 0.3 water to cement ratio and 10% air content.

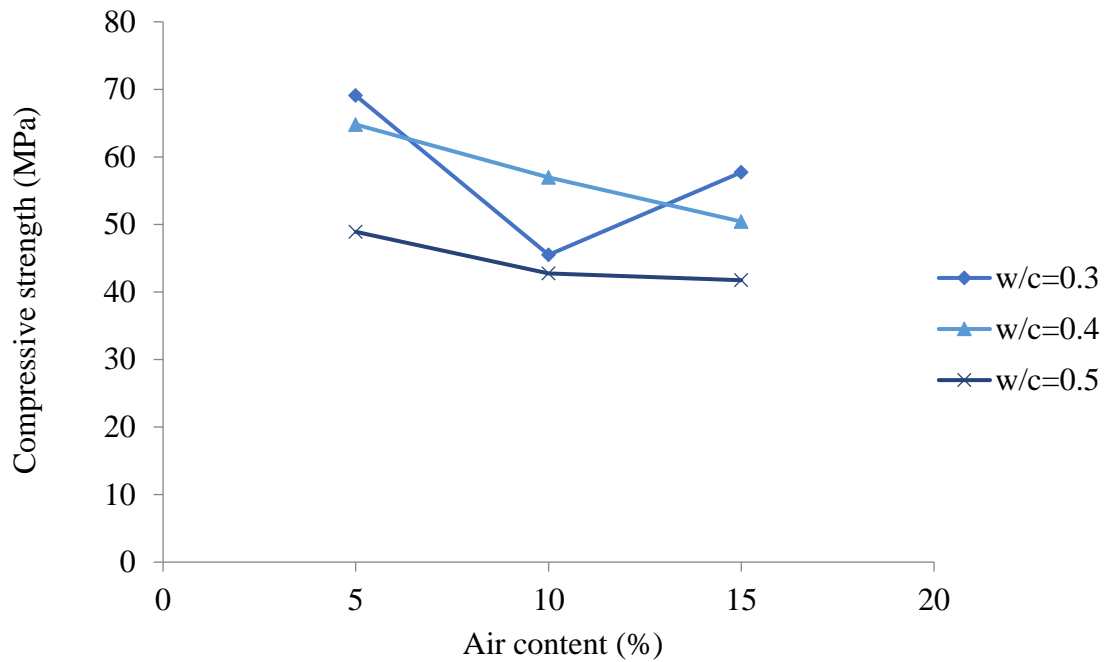


Figure 4.1. Compressive strength (MPa) – Air content (%) at room temperature

The load applied to the specimen that caused specimen to fail was recorded as residual compressive strength. Its absolute and relative values are shown in Figures 4.2 and 4.3. It is observed that all mixes have significant strength loss and the relationship between the percentage of voids and residual compressive strength is not clear. For specimens with 0.5 water to cement ratio, increasing air content leads to greater compressive strength loss, while specimens with 0.3 and 0.4 water to cement ratio do not show the similar trend. However, it could still be observed that specimens with 0.3 water to cement ratio and 5% air content has the highest residual

compressive strength while specimens with 0.5 water to cement ratio and 15% air content has the lowest residual compressive strength.

By considering relative values, it could be observed from Figure 4.3 that a higher air content leads to a higher compressive strength loss. One exception is specimens with 0.4 water to cement ratio and 5% air content.

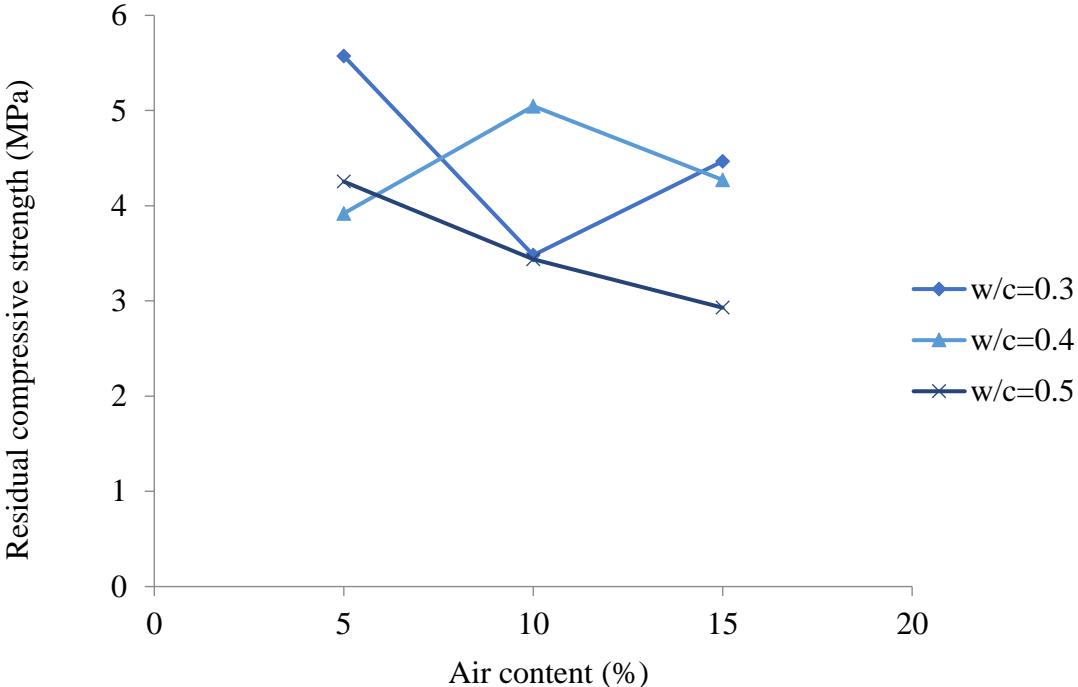


Figure 4.2. Residual compressive strength (MPa) – Air content (%) after heating

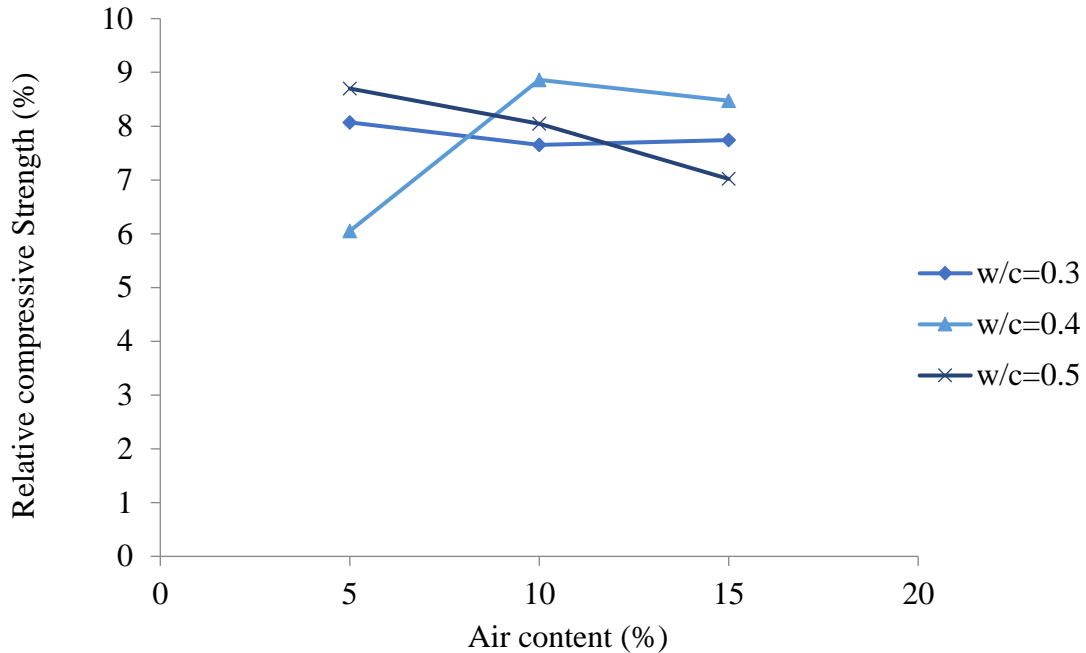


Figure 4.3. Relative compressive strength (%) – Air content (%) after heating

4.2 MASS LOSS

Concrete that is exposed to high temperatures will have a mass loss due to loss of water and presence of carbon dioxide (Bažant and Kaplan, 1996). The water inside concrete can be classified as three types: free water, physically and chemically bound water. When temperature reaches up to 100 °C, free water starts to change from liquid to vapor. Stress starts to build up inside capillary network and force this moisture escape from concrete microstructure. Coalescence of microstructural passages and high permeability created by air entrainment make it easy for vapor to escape and result in mass loss in this temperature range. After initial loss of free water, mass loss between 200 and 600 °C results mainly from loss of physically and chemically bound water. In 600 – 800 °C temperature range, decomposition of C-S-H gel and decarbonation of calcium carbonate generate water and carbon dioxide. Deterioration of concrete microstructure caused by high temperature helps the escape of vapor and affects mass loss. From Table 4.2, it could be

observed that mass loss varies slightly. The values vary from a minimum of 6.8% (mix 1) to a maximum of 9.8% (mix 12).

Table 4.2. Average mass loss values

Mixes	w/c	Void	Mass loss
		(%)	(%)
1	0.3	5	6.8
2	0.3	10	7.3
3	0.3	15	7.3
7	0.4	5	8.0
8	0.4	10	7.8
9	0.4	15	7.8
10	0.5	5	9.8
11	0.5	10	9.7
12	0.5	15	9.8

From Figure 4.4, it can be observed from the test data shown in Table 4.2, that specimens with the higher water to cement ratio have the greater mass loss. The reasonable explanation is that high water to cement ratio leads to high permeability which allows vapor to escape easily.

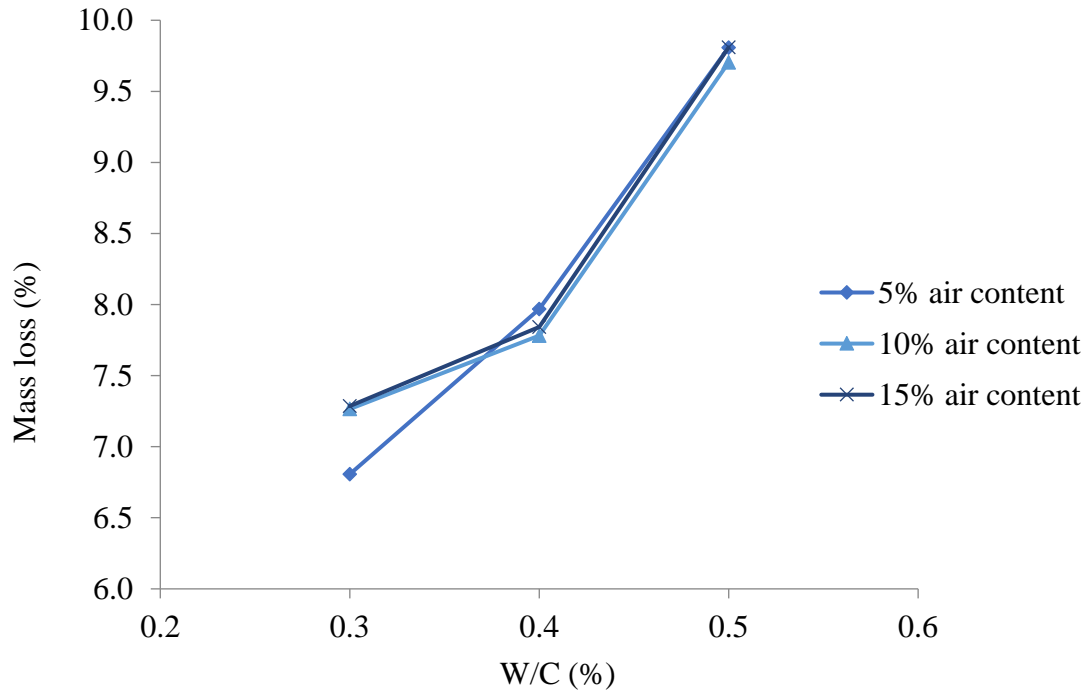


Figure 4.4. Mass loss (%) – w/c (%)

From Figure 4.5, it can be noticed that when considering the percentage of air voids, the relationship between air content and mass loss is not clear. For specimens with 0.3 water to cement ratio, it can be observed that specimens with 10% air content show greater mass loss than specimens with 5% air content, which could be attributed to larger air void system allowing more vapor to escape. However, specimens with 10% air content show a similar mass loss as specimens with 15% air content, which could be explained that after reaching a threshold, more air content addition does not have significant effect. For specimens with 0.4 and 0.5 water to cement ratio, the values are similar to each other.

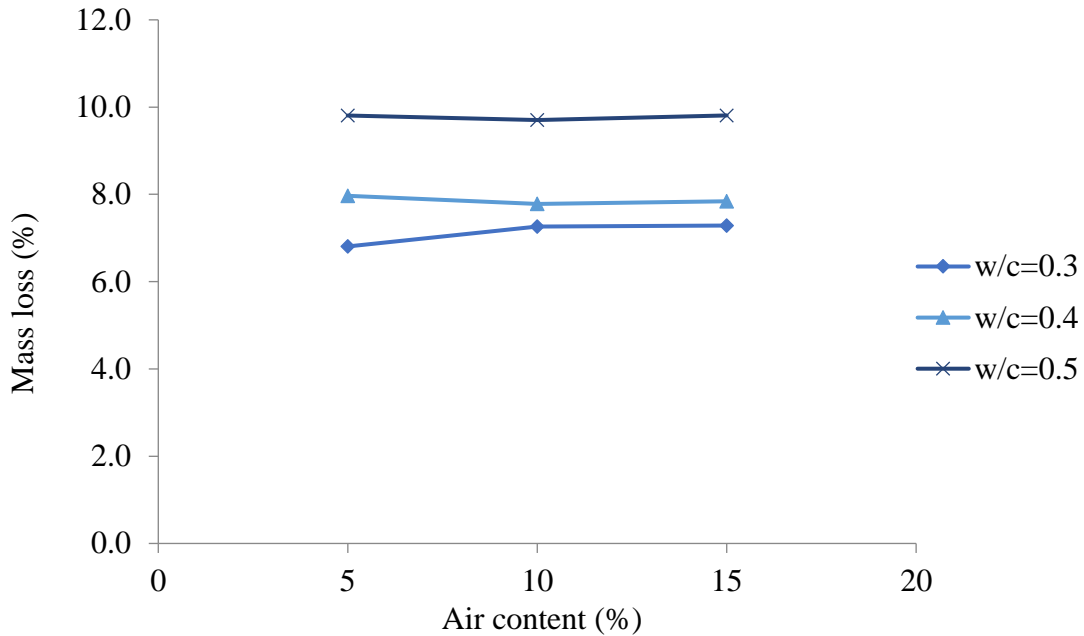


Figure 4.5. Mass loss (%) – Air content (%)

4.3 EFFECT OF PP FIBERS

Figures 4.6, 4.7 and 4.8 show the mass loss and residual compressive strength with or without PP fibers using the data in Table 4.3. It has been discussed that air entrainment affects the residual compressive strength of concrete. However, by comparing compressive strength data, it could be observed that the presence of PP fibers increases air void system's effect. All fibrous specimens show higher relative compressive strength than non-fibrous specimens.

Table 4.3. Average compressive strength and mass loss values

Mixes	w/c	Void (%)	Fiber (kg/m ³)	Initial strength		Residual strength			Mass loss (%)
				(MPa)	(psi)	(MPa)	(psi)	(%)	
1	0.3	5	0	69.1	10017.9	5.6	808.5	8.1	6.8
2	0.3	10	0	45.5	6598.3	3.5	504.9	7.7	7.3
3	0.3	15	0	57.7	8368.4	4.5	647.9	7.7	7.3
4	0.3	5	2	56.7	8220.5	4.9	704.0	8.6	7.3
5	0.3	10	2	68.3	9903.2	6.2	894.1	9.0	7.5
6	0.3	15	2	58.4	8476.0	5.7	830.9	9.8	7.5

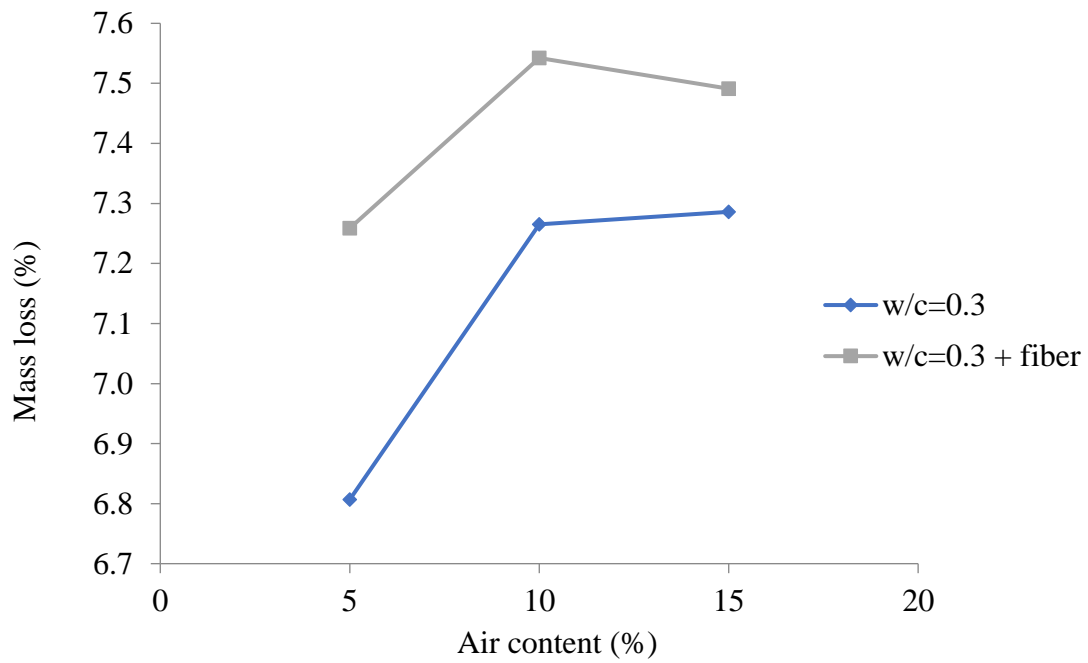


Figure 4.6. Mass loss (%) – Air content (%)

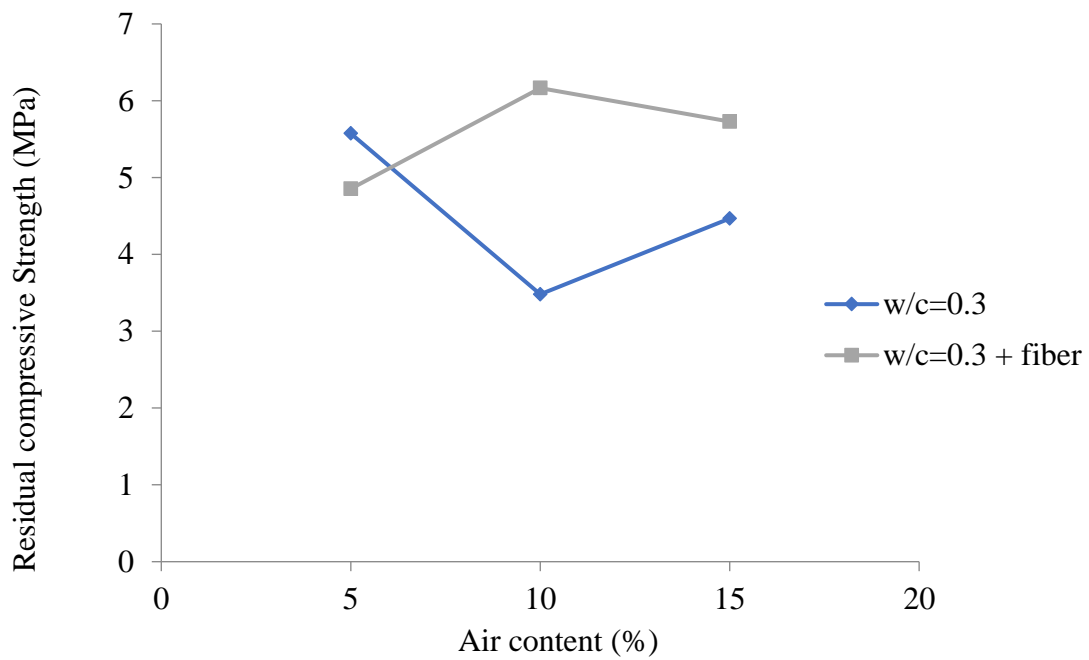


Figure 4.7. Residual compressive strength (MPa) – Air content (%) after heating

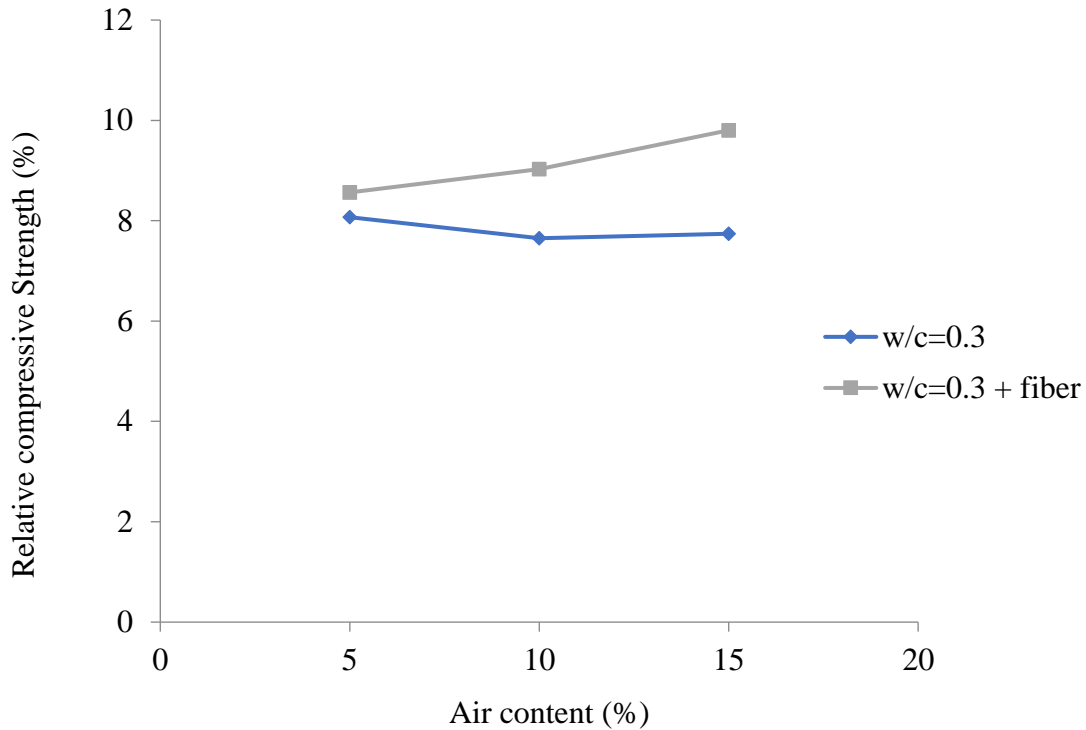
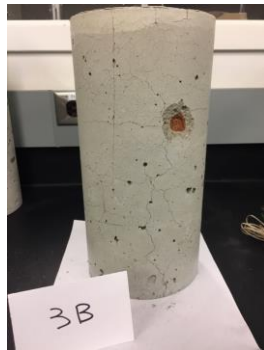
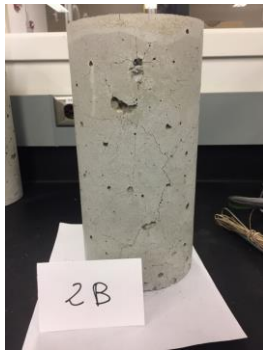
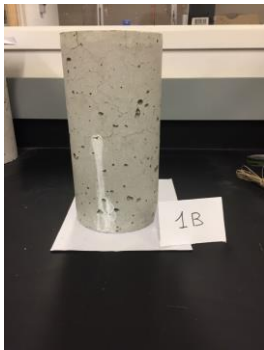
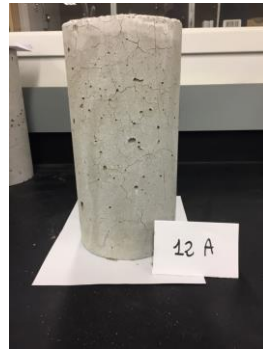
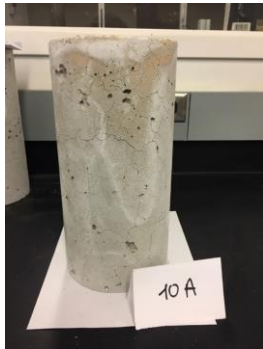
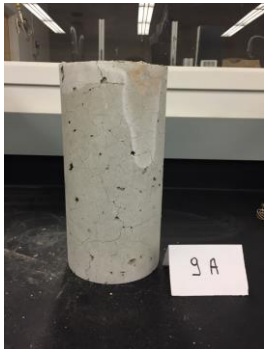
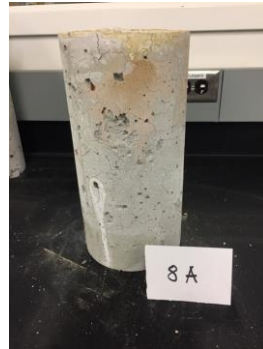
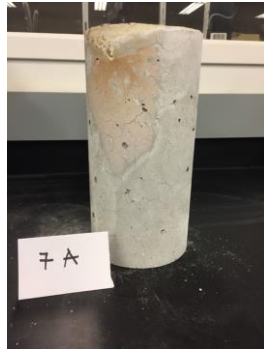
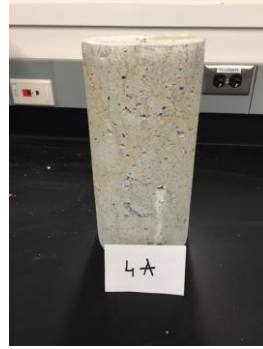
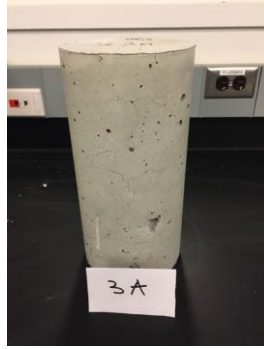
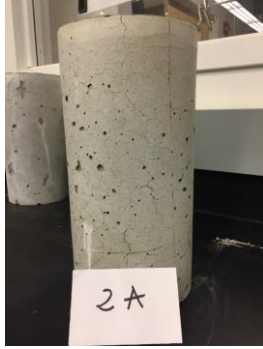


Figure 4.8. Relative compressive strength (%) – Air content (%) after heating

4.4 VISUAL OBSERVATION OF THE SPECIMENS

The visual observation of the specimens is of great importance as it could help identify the state of the specimens. Figure 4.9 are the photographs of specimens after they were taken out of the furnace. The first twelve are A series specimens and the others are B series specimens. It could be observed that the surface of all mixes changed to whitish gray. Akca and Zihnioglu (2013) stated that this phenomenon indicated that the temperature exceeded 600 °C and there was a serious compressive strength loss. This kind of deterioration is not repairable. Some specimens show pink surface. Ingham (2009) stated that this kind of discoloration was the result of hydrated iron oxides which happened around 300 °C. Some specimens (5A, 6A, 8A, 3B, 7B) subjected to split phenomenon and had brown inner surface. Small cracks could be observed in all specimens, but only specimen 12B showed deep cracks.



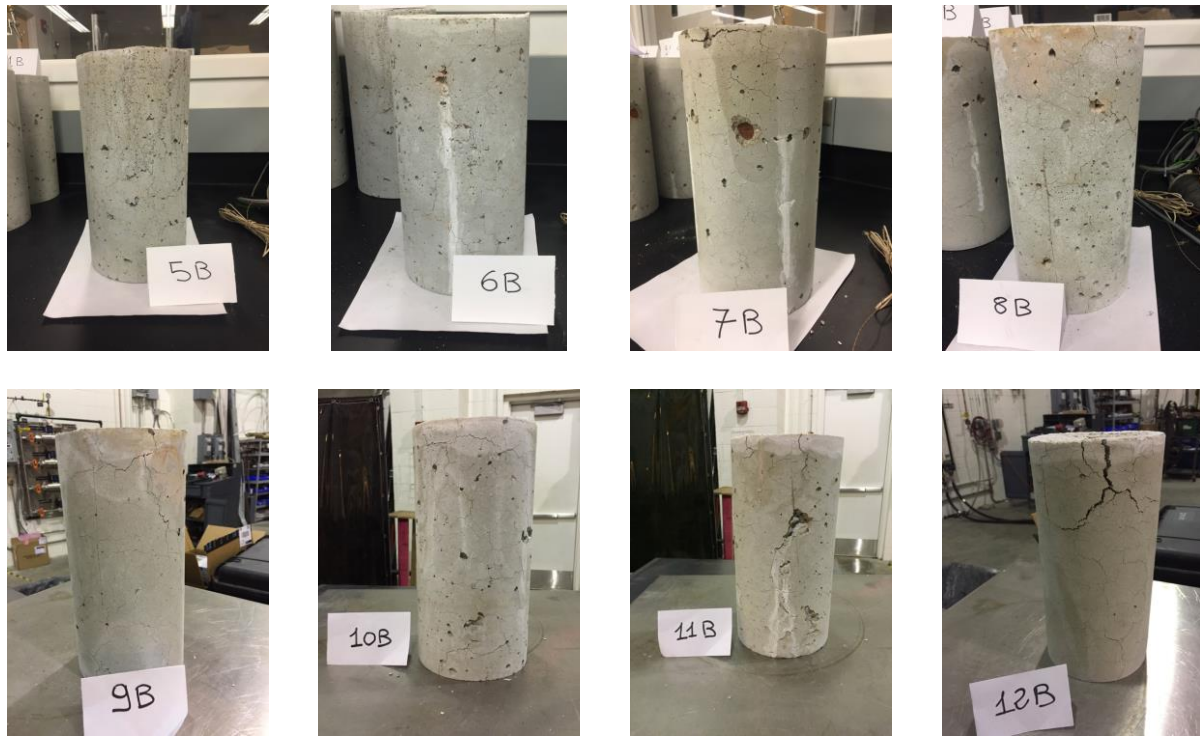


Figure 4.9. Photographic documentations of specimens after heating (Fantilli et al., 2018)

4.5 COMPARISON OF COMPRESSIVE STRENGTH AND MASS LOSS WITH OTHER STUDIES

To recognize air entrainment as an alternative method to reduce spalling, Waheed et al (2018) investigated air entrained HSC fire performance from 20 to 800 °C by controlling air content. Total of four mixes were prepared for this study. The first two were non-air entrained with 0.3 and 0.32 water to cement ratio (NAEH-1 and NAEH -2) and the other two were 0.3 water to cement ratio concrete with 4% and 8% air content (AEH-4 and AEH-8). Mechanical properties including compressive and splitting tensile strengths, stress-strain curve and elastic modulus were tested to evaluate the high temperature properties. Fire induced spalling, mass loss and internal cracking were observed to evaluate the physical properties.

Explosive spalling was observed at a temperature above 400 °C for NAEH-1 and 600 °C for NAEH-2. No spalling was observed for AEH-4 and AEH-8. The difference between NAEH-1 and NAEH -2 resulted from the difference in water to cement ratio. Higher water to cement ratio led to greater porosity, which helped NAEH -2 withstand higher temperature. The difference between NAEH and AEH could be attributed to air void system. With the help of well-distributed air voids, concrete could adapt to increased pressure caused by water changing from liquid to vapor which especially happened in the critical temperature range of 100 – 400 °C.

Internal cracking started between 200 and 400 °C in NAEH-2, which could be attributed to the dehydration of C-S-H gel and thermal expansion of aggregates. A higher amount of cracking is observed in NAEH-2 at 600 °C. In contrast, cracking started to be observed between 600 and 800 °C. High porosity help reduce cracking caused by thermo-mechanical processes, thermo-chemical changes, and vapor movement.

Spalling and cracking phenomenon were closely related to corresponding changes in strength and mass loss. With increasing temperature, these changes were observed at different rates.

By doing the comparison, it is noted that the residual values of concrete with 0.3 water to cement ratio have a similar trend. From Figures 4.10 and 4.11, AEH-8 shows higher loss in strength and mass than AEH-4. In our experiment, when the percentage of air void is around 5%, air entrained concrete has the highest relative residual compressive strength and lowest mass loss. If the air content becomes higher, specimens show greater mass and strength loss. With regards to mass loss, it could be said that higher air content help create a larger air void system which allows vapor to escape easily. However, greater mass loss is not always beneficial. According to Heo et al. (2012), when concrete loses more than 20% of the mass, spalling will be harmful.

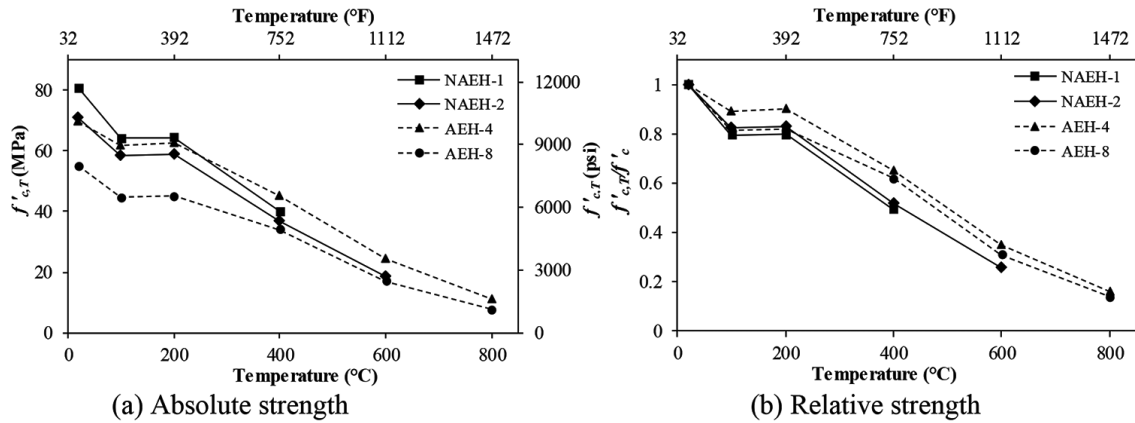


Figure 4.10. Variation in residual compressive strength as function of temperature (Waheed et al., 2018)

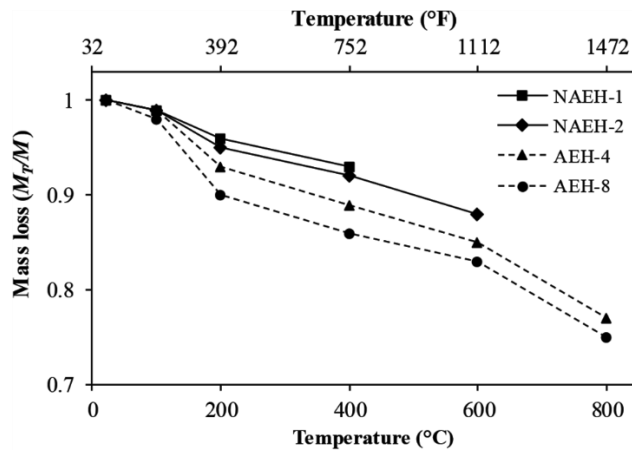


Figure 4.11. Relative mass loss after exposure to different temperatures in air and non-air entrained HSC (Waheed et al., 2018)

Akca and Zihnioglu (2013) investigated the combined effect of PP fibers and AEA on concrete fire resistance. Total nine mixes of HSC with 0.24 water to cement ratio were produced. F8 and F16 mixes represented the PP fibers to the volume of concrete are 8‰ and 16‰. A0, A0.5 and A1 mixes had AEA to cement ratio of 0‰, 0.5‰ and 1‰. Compressive strength, mass loss, macroscopic and microscopic observation were used to evaluate the properties of HSC at elevated temperature.

All mixes without fibers were exploded at 600 °C. No explosive spalling was observed when PP fibers were used except F8A0 (8‰ PP fibers to the volume of concrete ratio and 0‰ AEA to cement ratio) mixes. However, it should be noted that mixes with the same dosage of fibers and higher AEA (F8A0.5, F8A1) did not explode, which could be attributed to the effect of increasing air voids inside concrete.

Thermo Gravimetric Analysis (TGA) and Differential Thermo Gravimetry (DTG) curves were used to analysis mass loss (Figure 4.12). There were three peaks in DTG curves. The first represented the evaporation of moisture which appeared between approximately 20 and 150 °C. The second happened between approximately 400 and 450 °C which represented the loss of water from portlandite. The loss of carbon dioxide led to the third peak which appeared between approximately 550 and 700 °C.

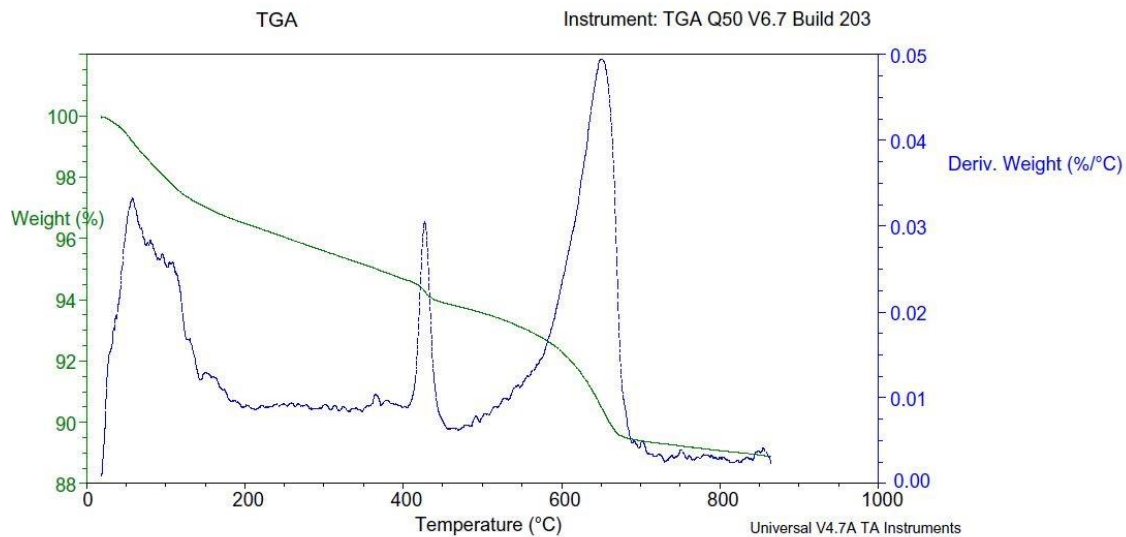


Figure 4.12. TGA and DTG curves (Akca and Zihnioğlu, 2013)

According to compressive strength test data, air entrained concrete had higher values. However, air entrained non-fibrous mixes exploded at 600 °C. This phenomenon could be

explained that with the help of microchannels formed by melted PP fibers, vapor inside air voids could escape easily and pore pressure went down. These results were similar to our data, as mixes with PP fibers addition have higher residual strength and mass loss in our experiment. It could be concluded that melted PP fibers create channels through air voids. The combination usage of PP fibers and air entrainment could provide a better effect on increasing fire resistance of concrete.

By doing the comparison, it is noted that the combination of PP fibers and AEA could be more effective against spalling. Differences exist when considering residual compressive strength. According to Akca and Zihnioğlu (2013), the existence of PP fibers has a negative effect on the residual strength of concrete while our experiment shows adding PP fibers has a positive effect on residual compressive strength.

Both Waheed et al (2018) and Akca and Zihnioğlu (2013) did microstructure observation. Waheed et al (2018) carried out scanning electron microscopy (SEM) investigation for both NAEH-2 and AEH-4. It can be inferred from the images that higher porosity of AEH-4 is beneficial to pore pressure dissipation as AEH-4 shows mostly crystalline morphology with less dense microstructure after being exposed to high temperature. Akca and Zihnioğlu (2013) examined microstructure of concrete by using an environmental scanning electron microscope (ESEM). It is confirmed from Figure 4.13 that PP fibers passed through air voids and micro-channels were formed.

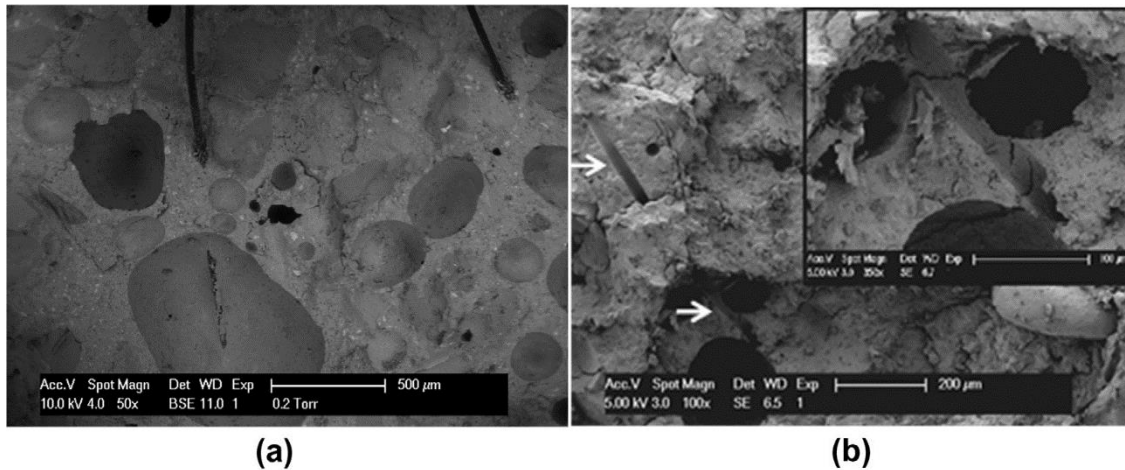


Figure 4.13. (a) A PP fiber passing through an air void, (b) a micro-channel formed after heating (a part of a melted PP fiber reaches to an entrained air void creating a micro-channel) (Akca and Zihnioğlu, 2013).

4.6 DISCUSSION

Considering the strange trend of initial compressive strength, there could be some flaws when casting concrete specimens. Therefore, mix 2 ($w/c = 0.3$, air void = 10%) is dismissed and corresponding figures are revised.

Revised compressive strength versus air content is shown in Figure 4.14. As expected, the compressive strength increases when air content and/or water to cement ratio decrease. Zhang et al. (2018) has reported this trend. They indicated that if the dosage of AEA was appropriate (air content of 4 – 5 %), compressive strength would not have noticeable decrease. if the air content exceeded 7%, compressive strength would suffer significant loss. This effect was more notable for concrete with low water to cement ratio. As the air content increases, concrete density will be reduced. If air content exceeds a certain range, air voids will substantially jeopardize compactness which causes compressive strength to decrease.

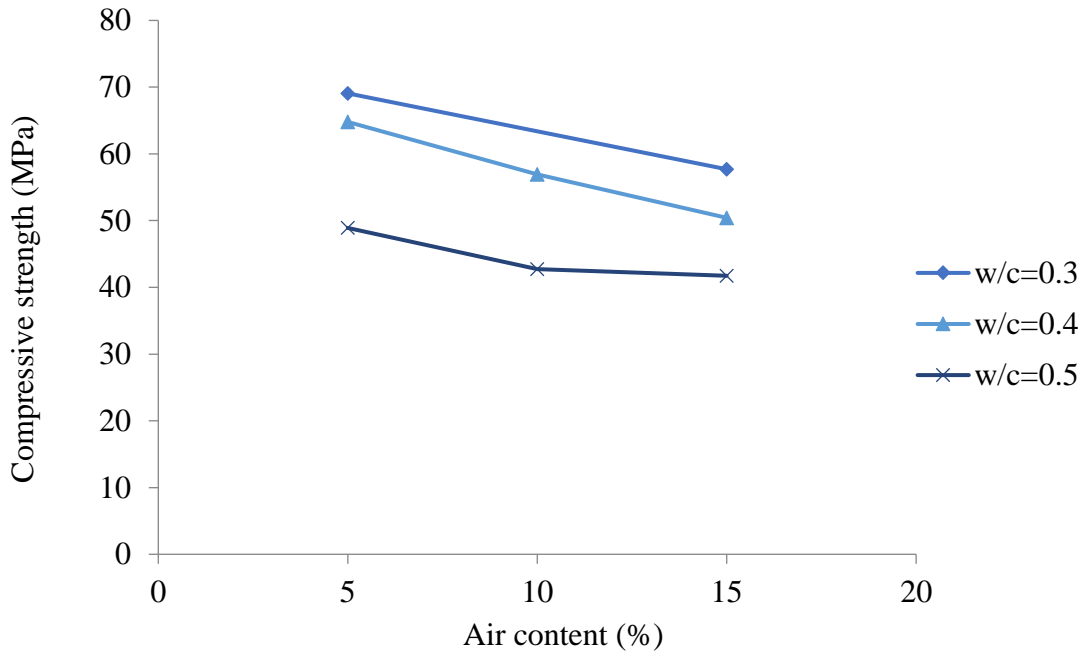


Figure 4.14. Compressive strength (MPa) – Air content (%) at room temperature

Both residual compressive strength and relative compressive strength versus air content are revised and shown in Figures 4.15 and 4.16. When the air content increases, residual compressive strength shows different trends if the water to cement ratios are different. For concrete with 0.3 and 0.5 water to cement ratio, 5% air content gives the highest residual compressive strength while 10% air content gives the highest residual compressive strength for concrete with 0.4 water to cement ratio. As noted by Waheed et al (2018), for each specific mix, there exists a specific dosage for AEA addition which could exactly provide place for all the generated vapors. If air content is lower than this dosage, an increase in air content could result in lower strength loss. If air content reaches this dosage, further increase is not beneficial and the effect of AEA addition against high temperature decreases.

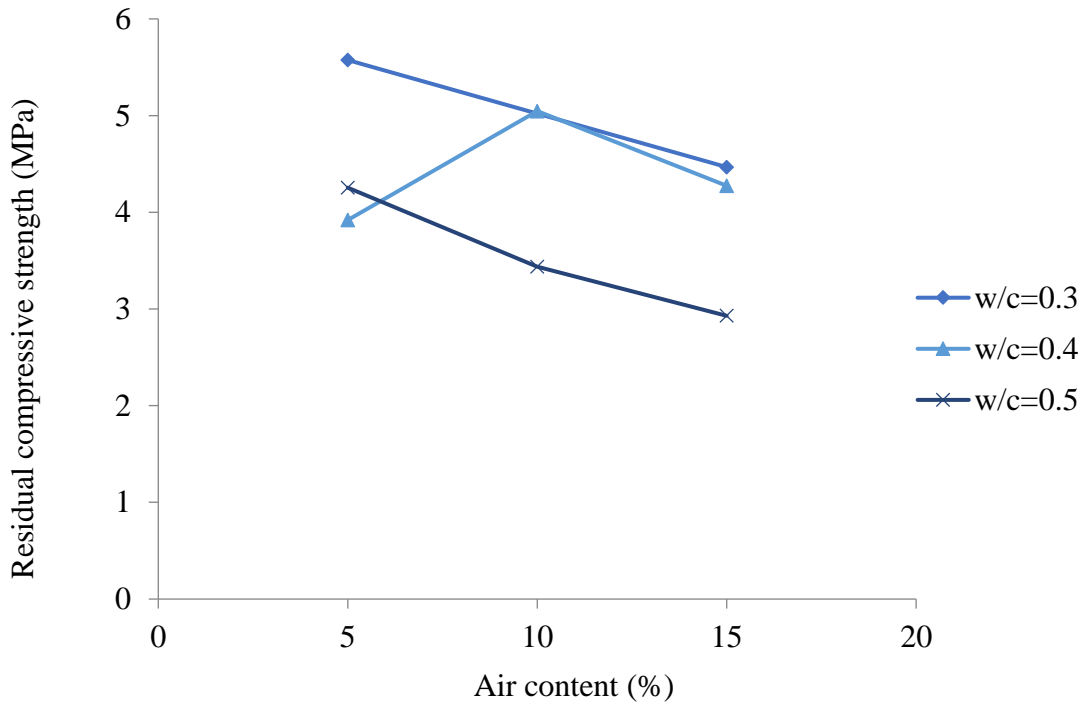


Figure 4.15. Residual compressive strength (MPa) – Air content (%) after heating

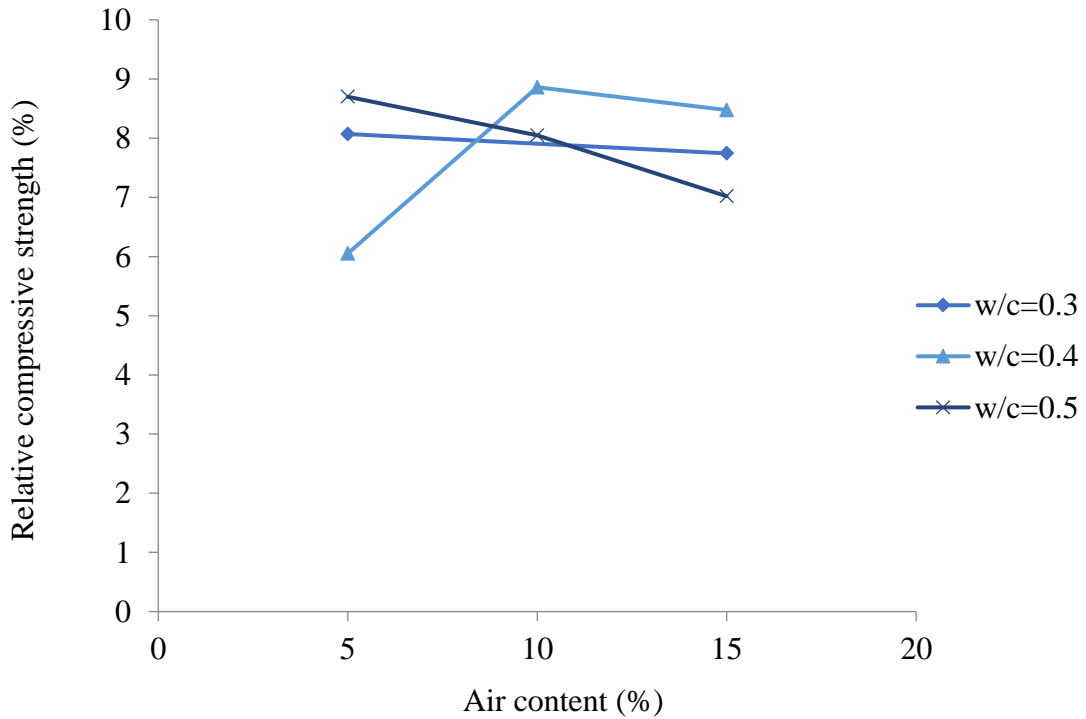


Figure 4.16. Relative compressive strength (%) – Air content (%) after heating

Revised mass loss versus air content is shown in Figure 4.17. It can be observed that mass loss increases slightly as air content increases when water to cement ratio is 0.3. On the other hand, however, mass loss does not have significant changes as air content increase when water to cement ratio is 0.4 or 0.5. This result is contrary to common opinion that air void system could allow vapors to escape. According to experiment carried by Waheed et al (2018), more air content leads to more mass loss and air entrained concrete has more than 20% mass loss. One possible explanation is that most air voids inside concrete just provide vacant place for vapor instead of helping transfer vapor from the core to the surface of concrete.

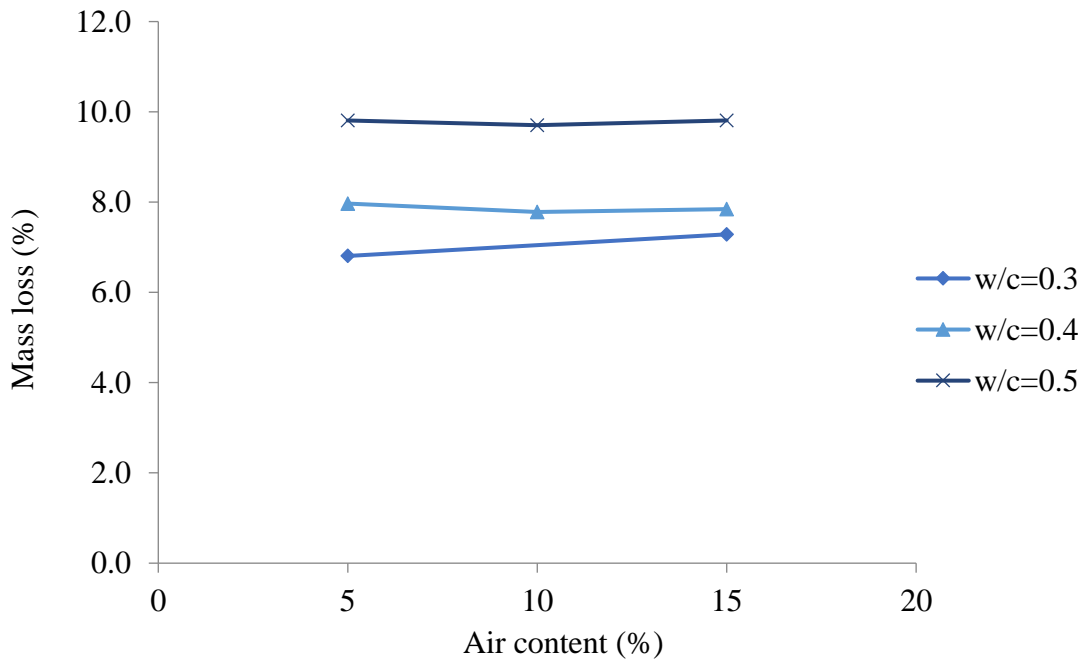


Figure 4.17. Mass loss (%) – Air content (%)

With regard to PP fibers, the results in our experiments show similar trend as other researchers. As noted by Akca and Zihnioğlu (2013), PP fibers addition increases the effect of air entrainment on increasing the fire resistance of concrete. Some air voids created by air entrainment are closed and not connected to each other, which causes the situation that vapor could not escape from these

closed voids as the pressure increases. As a result, the potential of spalling increases. As PP fibers melt at around 170 ° C, vacated channels are formed and help connect these air voids which make vapor escape from these voids easier. The effect of PP fibers helping vapor transport is also reported by Zeiml et al. (2006). They did experiment on normal concrete with and without PP fibers. By calculating the amount of vaporized and transported moles of water, they concluded that the amount of transported moles was greater than the amount of vaporized moles when PP fibers were added. However, the effect provided by PP fibers is not noticeable.

No explosive spalling is observed in all specimens which indicates that AEA and PP fibers could enhance resistance against spalling. These results are reported by other researchers (Waheed et al., 2018; Akca and Zihnioğlu, 2013; Ali and Talamona, 2004). Both air entrained and fibrous concrete has high porosity in hardened state. This high porosity gives concrete ability to adapt the phase changes of water. Therefore, the higher permeable the concrete is, the less the chance of explosive spalling is. Moreover, it is known that the thermal incompatibility between aggregates and cement paste could cause degradation of concrete microstructure. Well distributed air voids could absorb this incompatibility and mitigate spalling phenomenon.

Chapter 5. CONCLUSION AND RECOMMENDATION

The residual strength of concrete after being exposed to high temperature is important factor in concrete performance. Thus, the main objective of this thesis is to study the behavior of concrete exposed to high temperatures. The focus has been placed on whether precautions such as the addition of PP fibers and AEA could help decrease the damage when concrete is exposed to high temperatures. Compressive strength test, mass loss measurement and visual observation are used to evaluate the fire resistance of concrete. All the specimens show small mass loss that varies from a minimum 6.8% to a maximum 9.8%. On the contrary, the data obtained from the compressive strength tests show that all the specimens have great strength loss. The average residual compressive strength is 4.5 MPa while the minimum value is 2.56 MPa and the maximum value is 6.9 MPa. Only slight spalling phenomenon was observed in some specimens. These results show clearly that the addition of PP fibers and AEA increases permeability and this high permeability plays a significant role in allowing interior vapor to escape from concrete and reducing the fire damage. Based on the obtained results, the following conclusions are drawn:

1. Concrete heated to 1850 °F was nearly completely degraded.
2. Concrete with high water to cement ratio appears to undergo a high mass loss. The trend of mass loss shows positive correlation relationship with the water to cement ratio.
3. Concrete with high water to cement ratio appears to have a low residual compressive strength.
4. When air content is higher than 5 %, compressive strength decreases when air content increases.

5. The relationship between residual compressive strength and air content is not clear while it could be concluded that, for each specific mix, there exists an AEA dosage that could lead to highest residual compressive strength.

6. Mass loss does not change significantly when air content varies. More research is needed to determine whether AEA could help transfer vapor from the interior to the surface of concrete.

7. With the addition of PP fibers, air entrained concrete show better results after being exposed to high temperature. PP fibers improve AEA's positive effect. However, the effect is not noticeable.

8. AEA is effective in reducing spalling after exposure to fire.

Based on this study, it can be said that using AEA could help decrease the risk of spalling and combining PP fibers and AEA could be a more effective method. For future work, the fire test concrete specimens could be changed from unloaded to loaded and different time-temperature curves could be used to further evaluate the fire resistance of air entrained concrete.

BIBLIOGRAPHY

- Ali, F., Nadjai, A. & Talamona, D. (2004). Assessment of the susceptibility of normal and high strength concrete for explosive spalling. *Journal of applied fire science*, 13(1), 79-88.
- Akca, A. H. & Zihnioğlu, N. Ö. (2013). High performance concrete under elevated temperatures. *Construction and building materials*, 44, 317-328.
- ASTM E-119: Standard Test Methods for Fire Tests of Building Construction and Materials, ASTM International, Washington, D.C., 2018.
- Bažant, Z. P. & Kaplan, M. F. (1996). *Concrete at high temperatures: material properties and mathematical models*.
- Behnood, A. & Ghandehari, M. (2009). Comparison of compressive and splitting tensile strength of high-strength concrete with and without polypropylene fibers heated to high temperatures. *Fire Safety Journal*, 44(8), 1015-1022.
- Carette, G. G., Painter, K. E. & Malhotra, V. M. (1982). SUSTAINED HIGH TEMPERATURE EFFECT ON CONCRETES MADE WITH NORMAL PORTLAND CEMENT, NORMAL PORTLAND CEMENT AND SLAG, OR NORMAL PORTLAND CEMENT AND FLY ASH. *Concrete International*, 4(7), 41-51.
- Chan, Y. N., Peng, G. F. & Anson, M. (1999). Residual strength and pore structure of high-strength concrete and normal strength concrete after exposure to high temperatures. *Cement and concrete composites*, 21(1), 23-27.
- Cülfik, M. S. & Özturan, T. (2010). Mechanical properties of normal and high strength concretes subjected to high temperatures and using image analysis to detect bond deteriorations. *Construction and building materials*, 24(8), 1486-1493.
- Fantilli, A. P., Nemati, K. & Accornero, N. (2018). LO SPACCO ESPLOSIVO.
- Heo, Y. S., Sanjayan, J. G., Han, C. G. & Han, M. C. (2012). Limited effect of diameter of fibres on spalling protection of concrete in fire. *Materials and structures*, 45(3), 325-335.

- Ingham, J. P. (2009). Application of petrographic examination techniques to the assessment of fire-damaged concrete and masonry structures. *Materials characterization*, 60(7), 700-709.
- Khaliq, W. & Khan, H. A. (2015). High temperature material properties of calcium aluminate cement concrete. *Construction and Building Materials*, 94, 475-487.
- Khaliq, W. (2012). Performance characterization of high performance concretes under fire conditions (Vol. 73, No. 09).
- Khoury, G. A. (2008). Polypropylene fibres in heated concrete. Part 2: Pressure relief mechanisms and modelling criteria. *Magazine of concrete research*, 60(3), 189-204.
- Kodur, V. K. R. (2000). Spalling in high strength concrete exposed to fire: concerns, causes, critical parameters and cures. In *Advanced Technology in Structural Engineering* (pp. 1-9).
- Lea, F. C. (1920). The effect of temperature on some of the properties of materials. *Engineering*, 110(3), 293-298.
- Liu, J. C., Tan, K. H. & Yao, Y. (2018). A new perspective on nature of fire-induced spalling in concrete. *Construction and Building Materials*, 184, 581-590.
- Maluk, C., Bisby, L. & Terrasi, G. P. (2017). Effects of polypropylene fibre type and dose on the propensity for heat-induced concrete spalling. *Engineering Structures*, 141, 584-595.
- Mehta, P. & Monteiro, Paulo J. M. (2014). *Concrete : Microstructure, properties, and materials* (Fourth edition / P. Kumar Mehta, Paulo J.M. Monteiro. ed.). New York: McGraw-Hill Education.
- Mielenz, R. C., Wolkodoff, V. E., Backstrom, J. E. & Flack, H. L. (1958, July). Origin, Evolution, and Effects of the Air Void System in Concrete. Part 1-Etrained Air in Unhardend Concrete. In *Journal Proceedings* (Vol. 55, No. 7, pp. 95-121).
- Neville, A. (1963). *Properties of concrete*. New York: Wiley.
- Noumowé, A., Siddique, R. & Ranc, G. (2009). Thermo-mechanical characteristics of concrete at elevated temperatures up to 310 C. *Nuclear Engineering and Design*, 239(3), 470-476.

- Phan, L. T. (2008). Pore pressure and explosive spalling in concrete. *Materials and structures*, 41(10), 1623-1632.
- Pigeon, M., Plante, P. & Plante, M. (1989). Air void stability, Part I: Influence of silica fume and other parameters. *Materials Journal*, 86(5), 482-490.
- Poon, C. S., Azhar, S., Anson, M. & Wong, Y. L. (2001). Comparison of the strength and durability performance of normal-and high-strength pozzolanic concretes at elevated temperatures. *Cement and concrete research*, 31(9), 1291-1300.
- Rostasy, F. S., Weiß, R. & Wiedemann, G. (1980). Changes of pore structure of cement mortars due to temperature. *Cement and Concrete Research*, 10(2), 157-164.
- Sideris, K. K. & Manita, P. (2013). Residual mechanical characteristics and spalling resistance of fiber reinforced self-compacting concretes exposed to elevated temperatures. *Construction and Building Materials*, 41, 296-302.
- Siebel, E. (1989). Air-void characteristics and freezing and thawing resistance of superplasticized air-entrained concrete with high workability. *Special Publication*, 119, 297-320.
- Waheed, F., Khaliq, W. & Khushnood, R. A. (2018). High-Temperature Residual Strength and Microstructure in Air-Entrained High-Strength Concrete. *ACI Materials Journal*, 115(3).
- Zhao, J., Zheng, J. J., Peng, G. F. & van Breugel, K. (2017). Numerical analysis of heating rate effect on spalling of high-performance concrete under high temperature conditions. *Construction and Building Materials*, 152, 456-466.
- Zhang, P., Li, D., Qiao, Y., Zhang, S., Sun, C. & Zhao, T. (2018). Effect of air entrainment on the mechanical properties, chloride migration, and microstructure of ordinary concrete and fly ash concrete. *Journal of Materials in Civil Engineering*, 30(10), 04018265.

